

# Flight Path and Wing Optimization of Lithium-Air Battery Powered Passenger Aircraft

J. Michael Vegh\*, Juan J. Alonso†  
*Stanford University, Stanford, CA, 94305, U.S.A.*

Tarik H. Orra ‡, Carlos R. Ilario da Silva§  
*EMBRAER, São José dos Campos, SP, 12277-901, Brazil.*

The design of electric-powered aircraft for use in the commercial aviation sector is a complex, heavily multidisciplinary problem that requires careful consideration of power and energy tradeoffs, in addition to more traditional performance metrics. A multidisciplinary, multifidelity aircraft design code called SUAVE (Stanford University Aerospace Vehicle Environment) has been developed in part to address these considerations. This paper explores the application of this design code towards a passenger aircraft at the commercial scale, with the wing, flight path, and an electric propulsion system designed and optimized for a prescribed number of passengers at a variety of different ranges. Additionally, aircraft weight sensitivities to battery technology, motor technology, as well as takeoff and landing constraints were evaluated, and their relative feasibility assessed.

## Nomenclature

AoA	angle of attack
C	C rate the battery is discharged at
Esp	specific energy
f	factor in empirical discharge loss
F	Faraday Constant
$G_0$	Gibbs Free Energy
h	altitude
I	current
P	power
$P_{motor}$	motor power
Psp	specific energy
R	effective resistance
$R_0$	empirical resistance factor
$S_{ref}$	wing reference area
TOFL	Take Off Field Length
LFL	Landing Field Length
V	velocity magnitude
$V_0$	reaction potential
x	state of charge
$\alpha$	twist
$\Lambda$	sweep

---

\*Ph.D. Candidate, Department of Aeronautics & Astronautics.

†Associate Professor, Department of Aeronautics & Astronautics, AIAA Associate Fellow.

‡Aircraft Conceptual Design Engineer - Embraer, AIAA Senior Member.

§Technology Development Engineer - Embraer, AIAA Member.

Subscripts	
1,2,3...	segment number
rc	root chord
tc	tip chord

## I. Introduction

Fuel costs, along with demand for commercial air travel have been rising dramatically in the recent past. In particular, fuel costs have doubled over the past 10 years, having risen to account for approximately 50% of airline operating costs for wide-body airplanes and to 30% for regional jets.<sup>1</sup> Furthermore, demand is expected to increase by 1.4 to 3 times by 2025 from 2004 levels.<sup>2</sup> This increased demand for air travel will result in enormous additional greenhouse gas emissions, in the absence of substantial reductions in overall fuel burn.<sup>3</sup> Additionally, electric energy only costs a fraction of the equivalent amount of fossil fuel energy.<sup>4</sup> Therefore, the achievement of electrically-powered aircraft has powerful economic as well as environmental incentives.

As a result, there has been considerable interest in the design of electrically-driven aircraft, particularly in the case of fuel cells and batteries.<sup>5-7</sup> One of the primary advantages of batteries is due to the perceived relative lack of infrastructure required to implement vis. a vis. fuel cells, in particular, liquid hydrogen fuel cells. However, present-day battery technology does not allow for the development of commercial-scale all-electric aircraft, due to limitations in the specific energy, and in some cases specific power of lithium-ion batteries. Nonetheless, lithium-air batteries, initially, appear much more promising, with estimated specific energies ranging from 1000-2000 W-h/kg, and specific powers from .4-.67 kW/kg.<sup>8,9</sup> Lithium-air batteries were expected to be commercially available by 2030, although recent studies highlight significant design issues that may call this date into question.<sup>9,10</sup> One unique aspect of a lithium-air battery that must be taken into account in the design process is that, as the battery discharges, oxygen particles collect on the cathode, which in turn, causes the battery to gain mass.<sup>11</sup> For larger batteries (such as what may potentially be used for commercial aviation), this mass gain may be considerable.

## II. Methodology

Several issues must be examined in the design of an electric aircraft. Firstly, mass tends to be a primary metric of feasibility due to the fact that electrical components tend to be much heavier than their fossil fuel-based equivalents. Modern commercially available batteries in particular suffer from possessing a specific energy two orders of magnitude lower than Jet A ( $\sim 130$  W-h/kg vs. 12,000 W-h/kg, respectively).<sup>12</sup> Lithium-air batteries, are much more promising, particularly at the more optimistic specific energy estimate of 2000 W-h/kg. Unfortunately, this is still only 1/6 that of Jet A.

Nonetheless, several factors can improve the overall feasibility of these designs. Firstly, electrical systems tend to be more energy efficient than combustion-based systems. Thus, some of this gap in capability may be closed based on smaller energy conversion losses. Secondly, because much of the increased demand in air travel is at shorter ranges, electric aircraft need not be designed to match all of the capabilities of current commercial aircraft, and could meet this demand more easily by reducing the overall range. Thirdly, because battery-electric systems are thermodynamically different than standard combustion-based systems, the entire aircraft may be designed to fly at a lower altitude; commercial aircraft fly at the coldest part of the atmosphere primarily in order to improve the Carnot efficiency of the propulsion system; because a battery-motor-ducted fan based system is not a heat engine, there is no significant advantage to flying higher, at least from a strictly thermodynamic perspective. Thrust requirements for takeoff and landing may offset this, however, as the propulsor may grow with these requirements, which changes the optimal operating altitude from a propulsive standpoint.

Designing the aircraft for a lower altitude allows for the redesign of several of the aircraft components to reduce overall systems weight. For instance, because the pressure differential experienced by the fuselage is smaller at lower altitudes, the fuselage can be designed with less structural reinforcement, reducing the overall weight in cases where pressure loads dominate overall fuselage sizing structural requirements. Furthermore, due to the higher temperatures, the aircraft could operate at a lower Mach Number while maintaining

the same cruise velocity, reducing wave drag; thus, the wing may be unswept, which would also lower the structural weight. Finally, the increased freestream dynamic pressure on the aircraft allows for the wing and tail to be "shrunk," relatively speaking, which further decreases the overall aircraft weight.

In addition to energy constraints, one has to account for power constraints in designing electric aircraft. Lithium-air batteries, for instance, are expected to have a relatively low specific power, on the order of .67 kW/kg. One can significantly improve the feasibility of these designs by shaping both the flight profile and the wing to account for this.

To evaluate these designs and close on families of optima, the Stanford University Aerospace Vehicle Environment (SUAVE), was used. SUAVE is a multifidelity, multidisciplinary conceptual design tool that has been developed to address the evaluation, feasibility, and optimization of unusual aircraft designs, such as electric aircraft. SUAVE evaluates a given aircraft for a given mission by solving the equations of motion at a finite number of time steps based on mission constraints and prescribed aerodynamics and propulsion models.

The baseline aircraft evaluated here is a regional passenger jet, with a design payload of 114 passengers and design range of about 2400 nautical miles. This aircraft was chosen largely because, in the initial conceptual design process, it was thought that aircraft carrying a relatively smaller payload (as opposed to, for instance, a 747-class aircraft) would be easier to develop considering the significant weight penalties associated with even optimistic battery estimates.

In this study, the fuselage nose and tailcone ratios were reduced from 2 and 3 to 1.5 and 1.8 respectively (to reduce wetted area, which the lower operating altitude allows based on a lower drag divergence Mach Number<sup>13</sup>), while the turbfans and jet fuel were replaced with ducted fans, electric motors, and lithium-air batteries. Electric motor mass and ducted fan mass were estimated based on the state of the art (SoA) scaling correlation shown in Figure 1.<sup>14</sup>

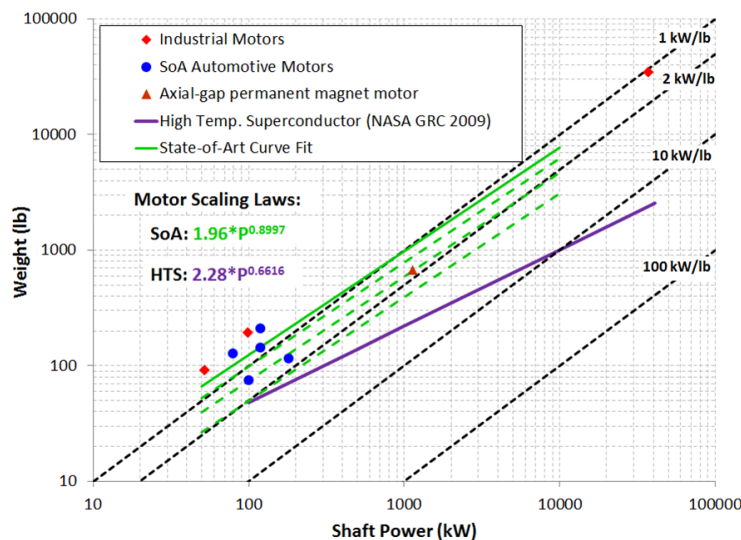


Figure 1: Electric Motor Scaling Correlation

Except when explicitly stated otherwise, all aircraft in this paper were designed using the state of the art (SoA) curve fit shown in Figure 1 to determine electric motor mass. Some interest has been shown in the relative weight gains one may experience using high temperature superconducting (HTS) motors, as they possess a considerable improvement in specific power, although their design and implementation is somewhat more complicated.<sup>5, 15</sup> This paper will also look at the potential gains in aircraft mass one can accomplish when they are optimized using the HTS motor fit shown in Figure 1. Boundary layer ingestion may result in additional efficiency gains.

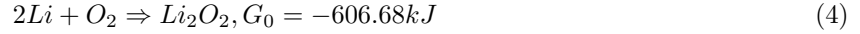
Battery discharge losses were modeled using an empirical discharge model developed in reference,<sup>16</sup> which is repeated below.

$$f = 1 - \exp(-20x) - \exp(-20(1 - x)) \quad (1)$$

$$R = R_0(1 + C \cdot f) \quad (2)$$

$$P_{discharge} = I^2 \cdot R \quad (3)$$

Additionally, the mass gain rate of the aircraft from battery discharge was based on the chemical reaction of lithium with oxygen, as seen below.<sup>9</sup>



$$\dot{m} = \frac{MW_{O_2}}{V_{0Li_2O_2} \cdot F} \cdot P \quad (5)$$

All other component weights were estimated based on traditional sizing correlations imported from PASS (Program for Aircraft Synthesis Studies) into SUAVE.<sup>17</sup> Aerodynamic properties were calculated via a weissinger vortex lattice method with profile drag correlations. The wing reference area, twist at the root and tip, sweep, and motor power were taken as input variables for an optimization scheme, while the taper and aspect ratio were maintained as equal to the baseline regional jet airplane (.28 and 8.3, respectively). The tail was sized based on a correlation from Raymer.<sup>18</sup> Furthermore, cruise velocity from the baseline aircraft was maintained. The cruise range as well as climb and descent profiles were also modified and optimized, based on a baseline flight profile with five climb segments and three descent segments. For the climb segments, the final altitude of each segment as well as the magnitude of the aircraft velocity at each segment were modified while maintaining the vertical climb rates; the mission solver then determined the throttle and angle of attack of the aircraft needed to match these parameters. Each descent segment maintained the baseline velocity magnitude and descent rate, while modifying the final segment altitudes, noting that the final segment altitude would always be sea level. Table 1 shows all of the design variables for the vehicle, while Table 2 depicts the flight profile design variables. Table 4 in the Appendix displays the vertical climb and descent rates along with the descent velocities, for reference.

Table 1: Aircraft Design Variables

$\alpha_{rc}$	$\alpha_{tc}$	$\Lambda$	$P_{motor}$	$S_{ref}$
---------------	---------------	-----------	-------------	-----------

Table 2: Mission Design Variables

$h_{climb_1}$	$h_{climb_2}$
$h_{climb_3}$	$h_{climb_4}$
$h_{climb_5}$	$V_{climb_1}$
$V_{climb_2}$	$V_{climb_3}$
$V_{climb_4}$	$V_{climb_5}$
$h_{descent_1}$	$h_{descent_2}$
<i>cruise range</i>	

An iterative scheme was developed to determine the maximum power required, along with the battery energy required to run the the mission based on the number of passengers, and aircraft component weights, including wing, battery and motor weights estimated for this particular aircraft and mission. Note that the battery accumulates a significant amount of weight throughout the mission; as a result, aircraft components were sized assuming a fully discharged battery, while the equations of motion took into account the increasing mass. The aircraft and mission were then optimized to determine the minimum possible landing weight. Design variables were constrained to ensure washout, maintain a target vehicle range, limit takeoff and landing field lengths, limit twist, as well as ensure consistency in the flight profile. The constraints can be seen below.

$$-5^\circ \leq \alpha_{tc} \leq \alpha_{rc} \leq 5^\circ \quad (6)$$

$$0^\circ \leq \Lambda \leq 30^\circ \quad (7)$$

$$0 \text{ km} < h_{climb_1} < h_{climb_2} < h_{climb_3} < h_{climb_4} < h_{climb_5} < 13 \text{ km} \quad (8)$$

$$h_{descent_1} > h_{descent_2} > 0 \text{ km} \quad (9)$$

$$-30^\circ \leq AoA \leq 30^\circ \quad (10)$$

$$TOFL \leq 1500m \quad (11)$$

$$LFL \leq 1500m \quad (12)$$

$$range \geq target \text{ range} \quad (13)$$

### III. Results

These aircraft, with proper initial guesses, allow for designs that may be somewhat comparable in weight to the baseline regional jet, depending on the range. Note that shaping the mission flight profile for these designs was crucial to ensure feasible weight breakdowns; it was found that merely replacing the propulsion system with a lithium-air based propulsion system, and running the same profile caused the sizing loop to diverge, largely due to the low specific power of lithium-air batteries. Choosing a new initial guess for the profile allowed for substantial reductions in gross landing weight. A CAD model of a representative electric aircraft (with a box representing the required battery volume) can be seen in Figure 2 below, along with a component weight breakdown, compared to the baseline in Figure 3.

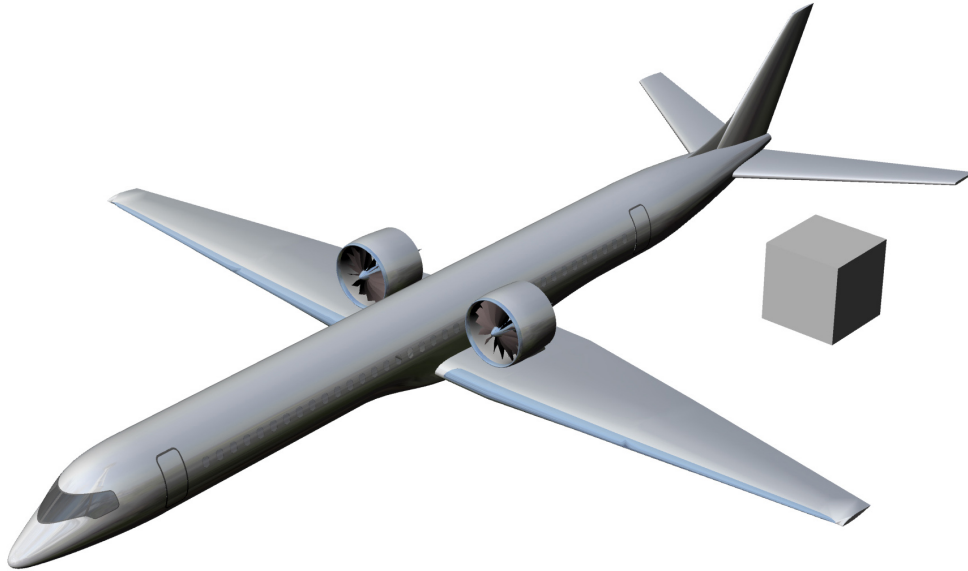


Figure 2: 4400 km Design (2000 W-h/kg .67 kW/kg battery)

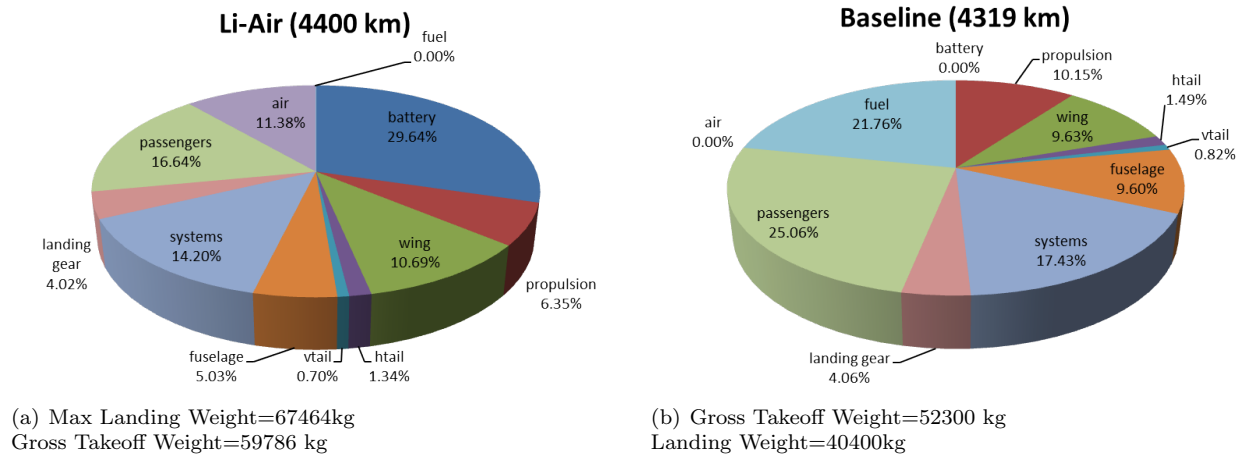


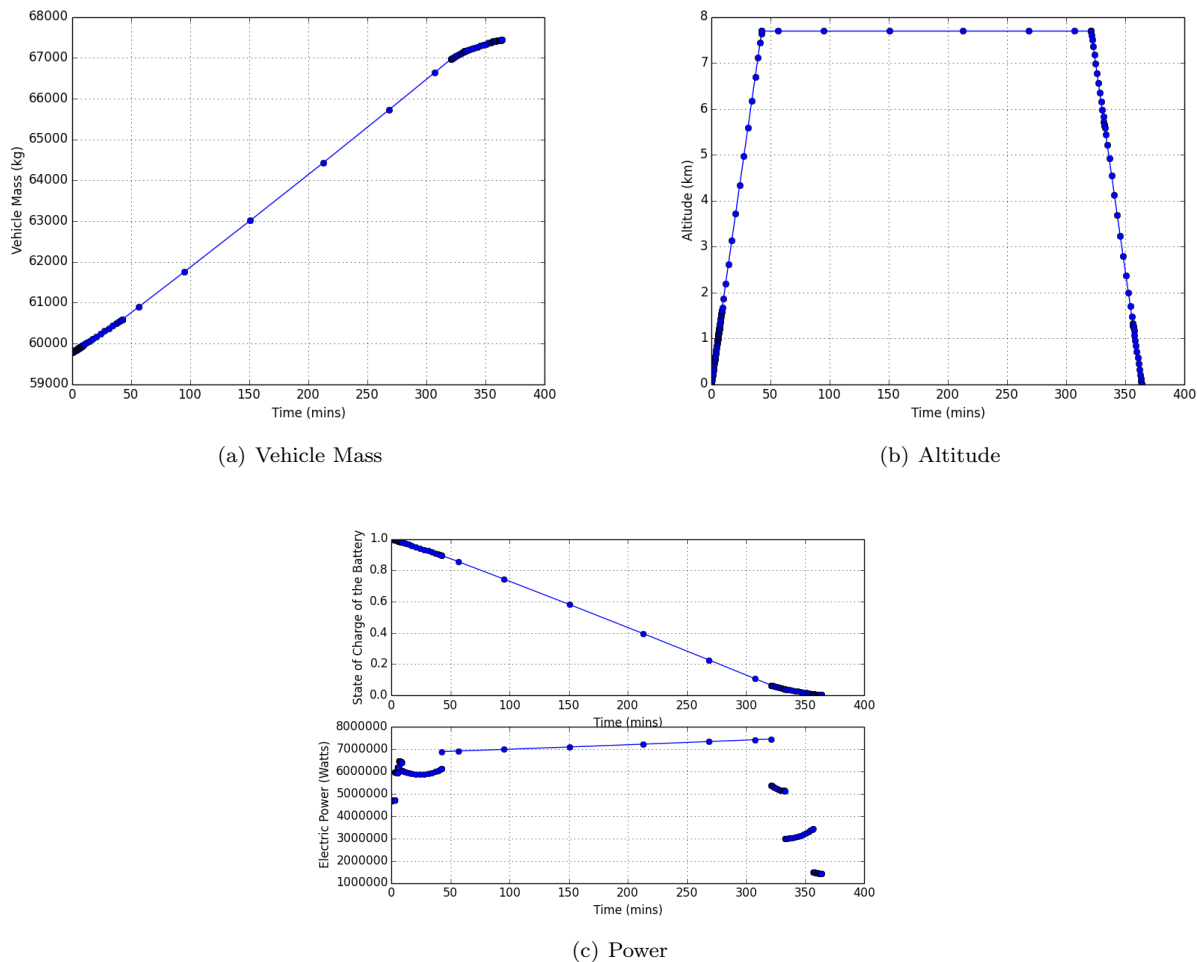
Figure 3: Weight Breakdown

It is immediately apparent that the battery takes up a very substantial portion of the aircraft, both from mass as well as volumetric standpoints, which must be taken into account for higher-level analysis and design. In particular, a blended-wing body design may be an effective solution to the apparent volumetric issues seen here. Note that the wing is completely unswept for this particular design. The fuselage is substantially lighter as well, comparably speaking (largely as a result of the lowered cruise altitude), which contributes to the overall feasibility of the design. Finally, one should bear in mind that distributed propulsion may lead to further reductions in weight; electric motor specific power is not particularly sensitive to scale. Thus, one may theoretically distribute ducted fans along the span of the wing to enable additional boundary layer ingestion benefits that are not currently modeled. Table 3 shows a comparison of the design variables for the baseline turbofan aircraft and an optimized electric aircraft.

Table 3: Aircraft Comparison

	Baseline Aircraft	Electric Aircraft (4400km)
$h_{climb_1}$	3.048 km	0.543 km
$h_{climb_2}$	3.657 km	0.994 km
$h_{climb_3}$	7.620 km	1.212 km
$h_{climb_4}$	9.754 km	1.601 km
$h_{climb_5}$	11.28 km	7.699 km
$h_{descent_1}$	9.31 km	5.631 km
$h_{descent_2}$	1.28 km	1.278 km
$V_{climb_1}$	138 m/s	125.5 m/s
$V_{climb_2}$	168 m/s	173.9 m/s
$V_{climb_3}$	200 m/s	180.9 m/s
$V_{climb_4}$	230 m/s	188.0 m/s
$V_{climb_5}$	230 m/s	178.4 m/s
$\alpha_{rc}$	2 °	-.322 °
$\alpha_{tc}$	0 °	-.341 °
$\Lambda$	22°	0.01 °
$S_{ref}$	92 m <sup>2</sup>	143.8 m <sup>2</sup>
<i>cruise range</i>	3426.2 km	3472.4 km
$P_{motor}$	N/A	7.45 MW

The tradeoffs between increased engine thrust, wing area, and field length were key in determining the final design of the electric aircraft; the cruise dynamic pressure of the electric design is 1.56 times that of the baseline aircraft, while the maximum mass of the aircraft is 1.25 times that of the baseline. Thus, in the absence of field length constraints, the wing area should be smaller. However, the landing mass is 1.67 times that of the baseline, due to the mass accumulation of the battery, which means that, to maintain landing field length requirements (Equation 12), the wing area needs to be increased. In addition, the optimizer determined that increased wing area carries a much smaller weight penalty than increased motor mass, so the takeoff field length constraint (Equation 11) also factored into the final designs. To maintain cruise efficiency, wing twist was decreased slightly. Furthermore, due to the lower Mach Number (.78 vs. .74), the wing became completely unswept. Note that the electric aircraft climbs at a much slower velocity to reduce power demands on the battery. Sample mission outputs from SUAVE for this particular design can be seen in Figure 4, while a flight profile of the baseline aircraft along with the electric version can be seen in Figure 5.



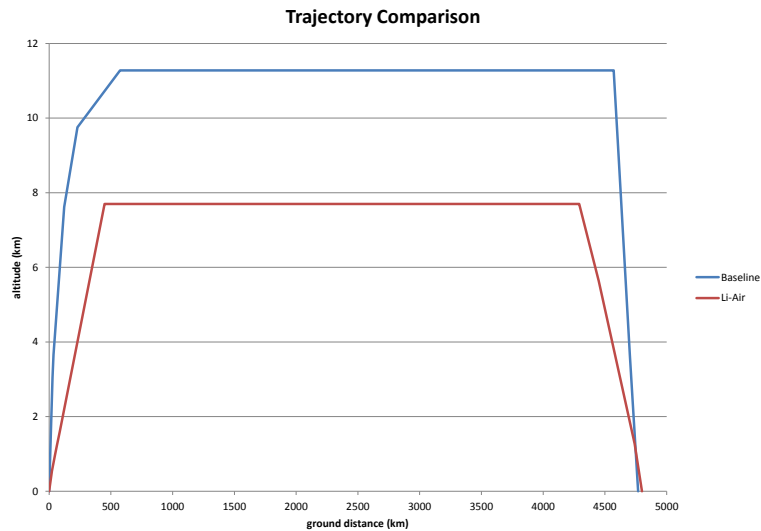


Figure 5: Aircraft Flight Profiles

These results show a number of interesting trends. Firstly, the cruise altitude is substantially lower than the baseline cruise altitude of 11.28 km, which enables the comparatively smaller fuselage weight shown in Figure 3. Secondly, note the relatively gentle power curve, especially when compared to that of the baseline, shown in Figure 10 in the Appendix, which again, was critical in ensuring convergence in the sizing loop. This trend can also be seen from the flight profile of the two vehicles, where the electric aircraft climbs and descends at a significantly lower rate than the baseline aircraft. Furthermore, battery mass accumulation has a significant impact on both power consumption, as well as in changing the angle of attack to maintain altitude and trim. Figure 6 depicts the landing weight, takeoff weight, as well as the baseline gross takeoff weight, highlighting the weight penalties for increasing the range.



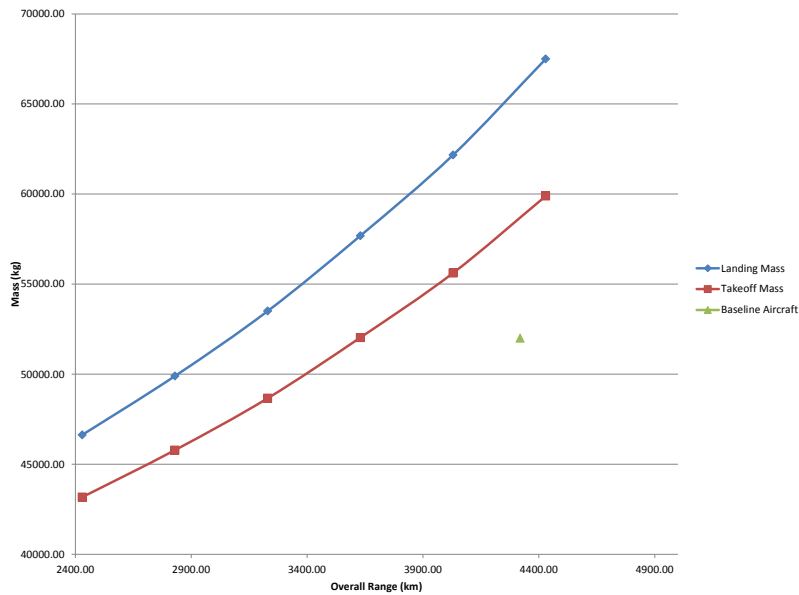


Figure 6: Aircraft Designs vs. Target Range

Of note here is that, particularly at shorter ranges, these electric aircraft have overall weights that compare favorably to the baseline aircraft. Furthermore, because much of the increased demand for commercial air travel is at shorter ranges, the design of these aircraft may be able to fill a niche role in the future aircraft market. However, with recent setbacks in lithium-air research, the 2000 W-h/kg specific energy value may be overly optimistic. Figure 7 shows a plot of landing weight of an optimized configuration vs design range at specific energies of 2000, 1500, 1000, 500, 250 W-h/kg, as well as a plot of 2000 W-h/kg designs with relaxed field length constraints.

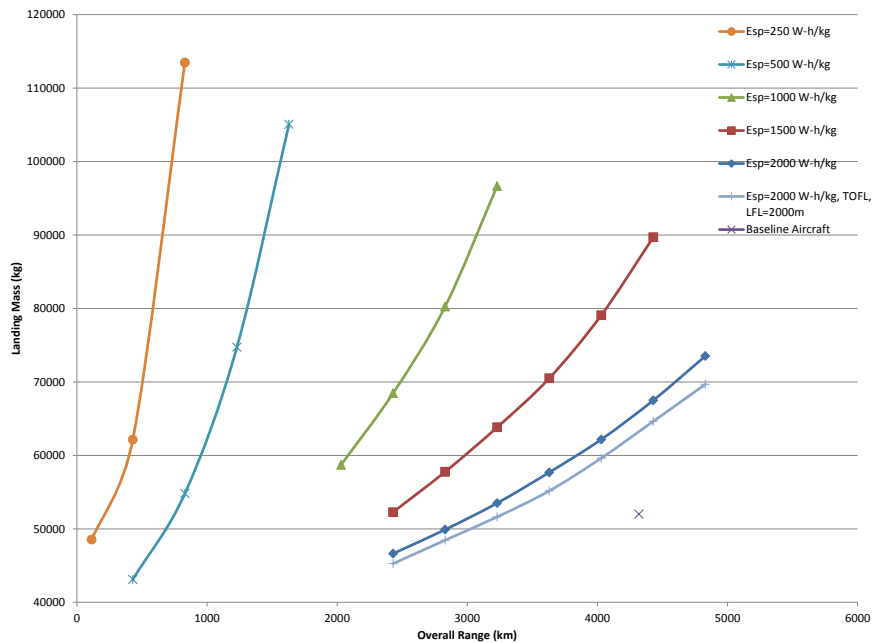


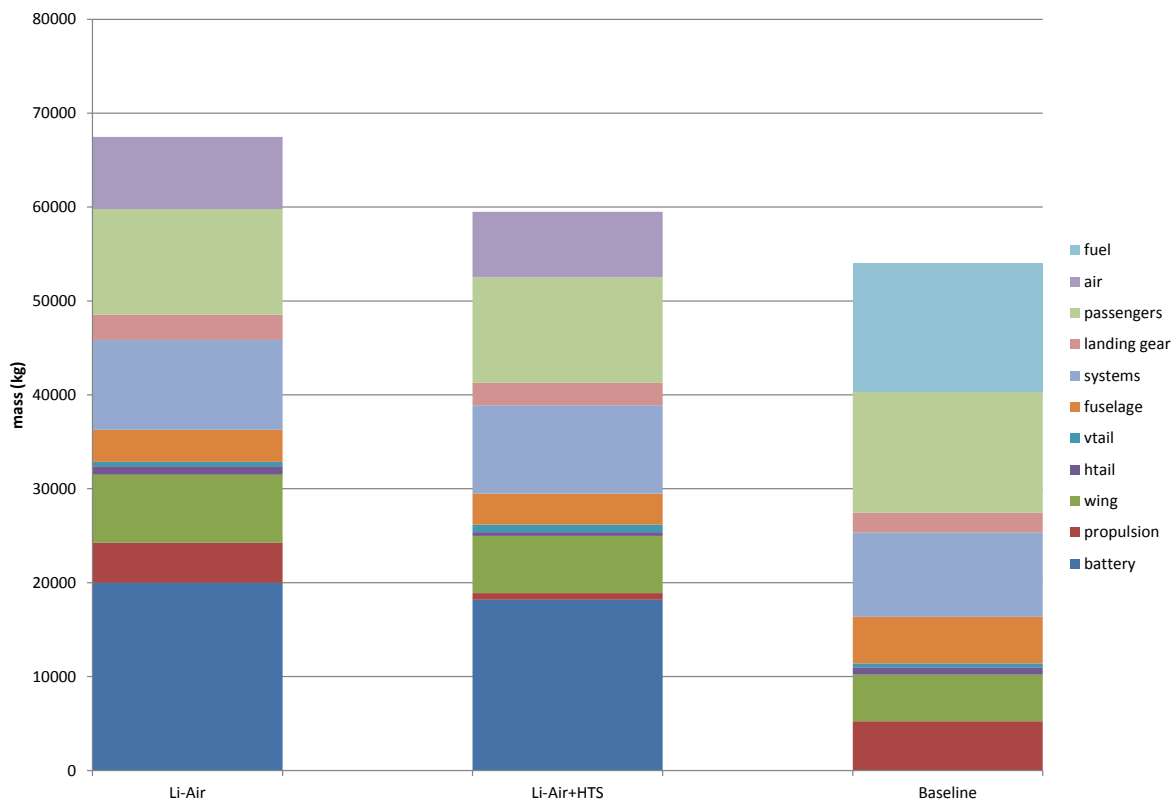
Figure 7: Battery Technology Comparison

Figure 7 illustrates that decreasing the design range of these aircraft may allow for feasible designs, even using existing (or at least near-term) battery technology. Nonetheless, one should note the substantial weight penalty associated with lower specific energy batteries. Furthermore reducing the number of passengers is recommended for these very short range aircraft (e.g.  $E_{sp}=500$  W-h/kg, range=430 km), and the designer would likely start with a “clean sheet” approach.

Additionally, the plot illustrates that, when the field length constraint is relaxed, some weight gains can be seen, although to a smaller extent than one might expect. In this case, the optimizer lowers the wing surface area, which decreases drag at cruise, but this is offset by the fact that the higher surface area allows for a much slower climb rate (noting that  $P \propto V^3$ ). At longer design ranges, relaxation of this constraint achieves additional mass gains, as the climb segment becomes a smaller fraction of the overall mission.

Interestingly, as the specific energy of the battery decreases, the difference in specific energy between fully charged and discharged batteries becomes less significant, as shown in Figure 9 in the Appendix. As a result, the 250 W-h/kg designs also approximate the performance of aircraft designed using more conventional battery chemistries at that specific energy (such as state of the art lithium-ion, or lithium-sulfur batteries).

On the other hand, these aircraft configurations were designed assuming no other technology improvements, which could lead to further weight reductions if well implemented. Additional optimization while factoring in advanced technology such as laminar flow, boundary layer ingestion, and composites, should yield considerably more improvement. Figure 8 shows the effect of designing the aircraft using superconducting motors at the 4400 km range, increasing the motor efficiency from 95 % to 99 % while using the superconducting motor sizing correlation from Figure 1.



1

Figure 8: Electric Technology Comparison

Figure 8 compares the component weight breakdown of an air-cooled-motor based design, an HTS-motor design, as well as the baseline aircraft. This chart illustrates that substantial gains can be made in the design

of these aircraft based on technology improvement. Notably, the takeoff weight of the HTS design is actually lighter than the gross takeoff weight of the baseline (52,500 kg vs 54,000 kg). More aggressive configuration changes, as well as the inclusion of composites could further improve feasibility, and are worthwhile topics for follow up studies.

## IV. Conclusions

Electrically-driven aircraft at the regional jet scale appear somewhat promising, at least in the initial conceptual design stages, when using these advanced batteries. Moreover, due to the fact that much of the increased demand for commercial aviation is at shorter mission ranges, lighter, shorter-range aircraft may be able to find a niche in the growing market. Furthermore, the introduction of more unconventional concepts, including blended-wing-body designs, coupled with distributed propulsion and boundary layer ingestion could result in substantial additional mass gains. However, looking forward, there are a number of questions that need to be addressed in follow-up studies to gain a more complete understanding of the feasibility of these aircraft. Firstly, analysis on the potential benefits of charging the battery directly vs. designing the battery to be easily removable and replaced with a fully charged one at the airport must be considered. Secondly, battery mass accumulation is likely to change the center of gravity of the aircraft, which could change the aerodynamic characteristics considerably, and needs to be addressed via solid geometry modeling. Thirdly, thermal losses, and their role in the overall electric system efficiency should be addressed. Finally, economic trade studies need to be undertaken to compare the costs/benefits of operating these aircraft based according to an assumed cycle-life of lithium-air batteries. Work is ongoing in refining the modules and investigating how the incorporation of additional technologies, such as distributed propulsion and boundary layer ingestion, affect the overall shape of the design.

## References

- <sup>1</sup>Boeing Commercial Airplanes, "Current Market Outlook: 2012-2031," <http://www.boeing.com/cmo>, 2012.
- <sup>2</sup>JPDO, "Next Generation Air Transportation System - Integrated Plan," Technical Report, Joint Planning and Development Office (JPDO), 2011.
- <sup>3</sup>"Intergovernmental Panel on Climate Change," <http://www.ipcc.ch/>, Accessed: May 2014.
- <sup>4</sup>Moore, M. and Fredericks, B., "Misconceptions of Electric Propulsion Aircraft and their Emergent Aviation Markets," *AIAA SciTech*, NASA Langley Research Center, National Harbor, Maryland, 2014.
- <sup>5</sup>Snyder, C., Berton, J., Brown, G., and et all, "Propulsion Investigation for Zero and Near-Zero Emissions Aircraft," *NASA STI Program*, NASA Glenn, 2009.
- <sup>6</sup>Ashcroft, S., Padron, A., Pascioni, K., Stout, G., and Huff, D., "Review of Propulsion Technologies for N+3 Subsonic Vehicle Concepts," NASA Glenn Research Center, 2011.
- <sup>7</sup>Hepperle, M., "Electric Flight- Potential and Limitations," German Aerospace Center, 2012.
- <sup>8</sup>Johnson, L., "The Viability of High Specific Energy Lithium Air Batteries," Tech. rep., Excellatron Solid State LLC., Oct. 2010.
- <sup>9</sup>Stückl, S., van Toor, J., and Lobentanzer, H., "Voltair: The All Electric Propulsion Concept Platform-a Vision for Atmospheric Friendly Flight," *28th International Congress of the Aeronautical Sciences*, EADS, 2011.
- <sup>10</sup>"Two big labs step back from the most promising next-generation battery," Quartz, May 2014, Accessed: September 2014.
- <sup>11</sup>Bruce, P., Freunberger, S. A., Hardwick, J. J., and Tarascon, J. M., "Li-O<sub>2</sub> and Li-S batteries with High Energy Storage," *Nature Materials*, Vol. 11, No. 1, 2012.
- <sup>12</sup>"Tesla Model S Facts," <http://www.teslamotors.com/models/facts>, Accessed: Jul. 2013.
- <sup>13</sup>I. Kroo, R. S., "AA241A Course Notes: Aircraft Design, Synthesis and Analysis," <http://adg.stanford.edu/aa241/AircraftDesign.html>, Accessed: Nov. 11, 2014.
- <sup>14</sup>Sinsay, J., Tracey, B., Alonso, J., Kontinos, D., Melton, J., and Grabbe, S., "Air Vehicle Design and Technology Considerations for an Electric VTOL Metro-Regional Public Transportation System," *12th AIAA Aviation Technology, Integration, and Operations (ATIO) Conference and 14th AIAA/ISSMO Multidisciplinary Analysis and Optimization Conference*, AIAA, Indianapolis, IN, 2012.
- <sup>15</sup>Luongo, C., Masson, P., Nam, T., and et. all, "Next Generation More-Electric Aircraft: A Potential Application for HTS Superconductors," *IEEE Transactions on Applied Superconductivity*, 2009.
- <sup>16</sup>Datta, A. and Johnson, W., "Requirements for a Hydrogen Powered All-Electric Manned Helicopter," NASA Ames Research Center, Moffett Field, CA, 2011.
- <sup>17</sup>Kroo, I., "An Interactive System for Aircraft Design and Optimization," *AIAA 1992-1190*, Aerospace Design Conference, Irvine, CA, 1992.
- <sup>18</sup>Raymer, D., *Aircraft Design: A Conceptual Approach*, AIAA, Playa del Ray, California, 4th ed., 2006.

## V. Appendix

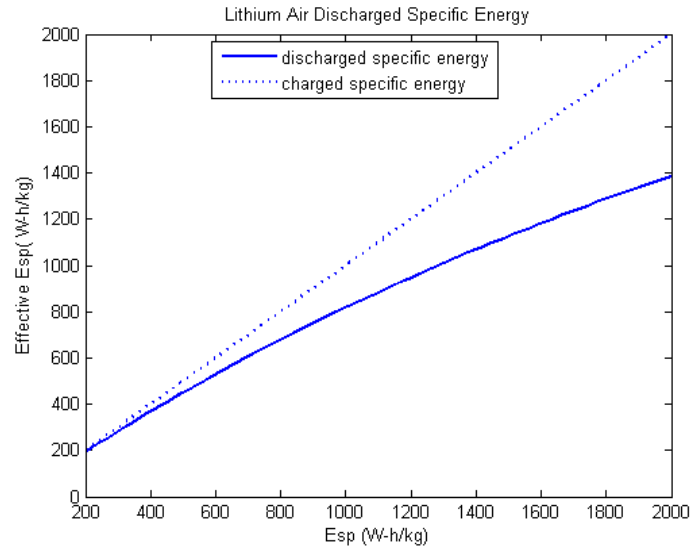


Figure 9: Lithium Air Discharged Specific Energy

Table 4: Flight and Descent Trajectories

$\dot{h}_{climb_1}$	10.16 m/s
$\dot{h}_{climb_2}$	7.62 m/s
$\dot{h}_{climb_3}$	7.62 m/s
$\dot{h}_{climb_4}$	4.572 m/s
$\dot{h}_{climb_5}$	1.016 m/s
$\dot{h}_{descent_1}$	8.128 m/s
$\dot{h}_{descent_2}$	7.62 m/s
$\dot{h}_{descent_3}$	7.62 m/s
$V_{descent_1}$	230 m/s
$V_{descent_2}$	200 m/s
$V_{descent_3}$	140 m/s

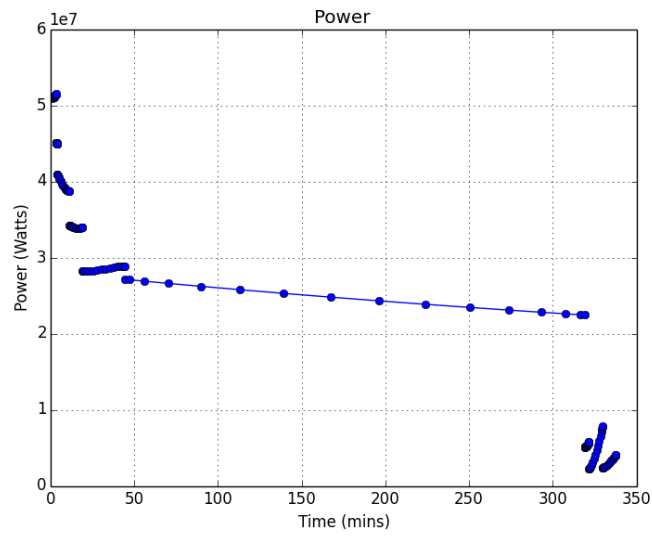


Figure 10: Baseline Power Profile

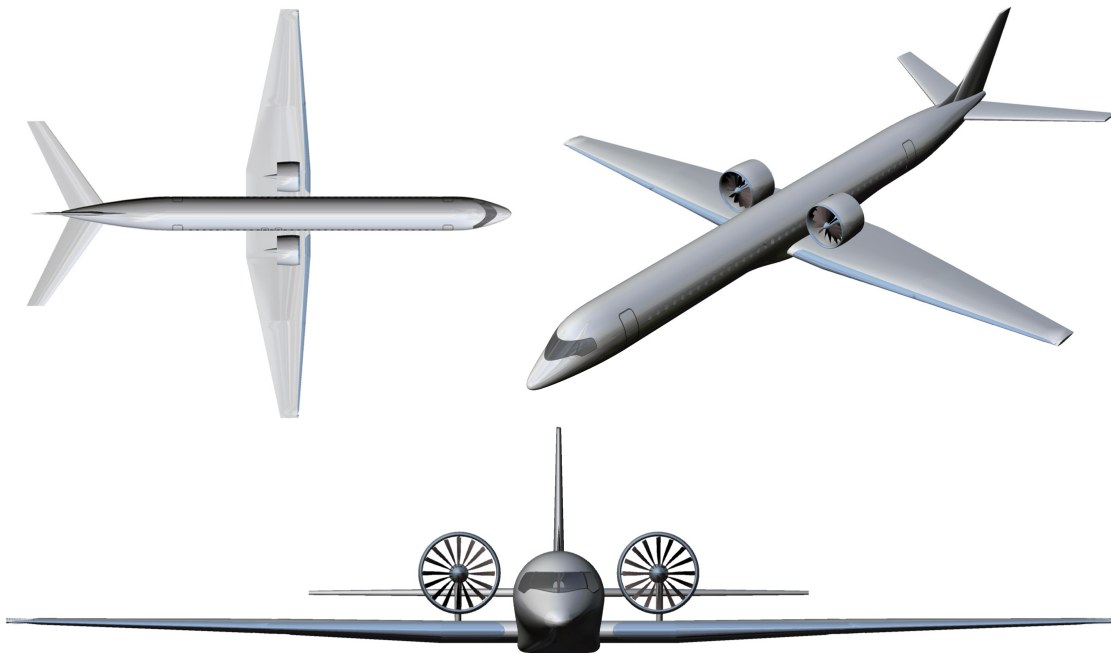


Figure 11: Aircraft Models